Compositional ordering and phase transitions in $Pb(Yb_{0.5}Nb_{0.5})O_3$

1993 J. Phys.: Condens. Matter 5 5491

(http://iopscience.iop.org/0953-8984/5/31/013)

J. Phys.: Condens. Matter 5 (1993) 5491–5504. Printed in the UK

Compositional ordering and phase transitions in $Pb(Yb_{0.5}Nb_{0.5})O_3$

A A Bokov, V Y Shonov, I P Rayevsky, E S Gagarina and M F Kupriyanov
Rostov State University, Rostov-on-Don 344104, Russia

Received 5 January 1993, in final form 26 March 1993

Abstract. The possibility of varying the compositional long-range order parameter s and the influence of s on the ferroelectric properties of pure and Li-doped $Pb(Yb_{0.5}Nb_{0.5})O_3$ ceramics have been studied. X-ray diffraction and dielectric measurements were used. A compositional order–disorder phase transition was discovered at 1120 °C (in doped ceramics). It was shown that in the course of material synthesis the compositionally ordered perovskite structure is formed at comparatively low temperatures (800 °C) and the s value may be reduced during sintering at higher temperatures. The pure ceramic remains ordered after sintering because the rate of s change in it is much lower than in the doped material. Low-temperature sintered doped ceramics are characterized by spatial non-homogeneities of s, causing the appearance of two (or more) anomalies in the temperature dependence of the permittivity. The T–s phase diagram has been investigated. Materials with a low s ($s < s_c$) show a diffuse transition from high-temperature paraelectric phase to ferroelectric phase (at $T_C = 115$ °C when $s = 0$). For materials with a high s ($s > s_c$) a paraelectric to antiferroelectric phase transition is observed. Thus there is a triple point at $s = s_c$. The Curie temperature T_C is quadratic in s and a minimum in the $T_C(s)$ curve is observed at the triple point, which is in agreement with the earlier theoretical treatment of Bokov *et al*.

1. Introduction

Compositional ordering, i.e. variation of the order present between ions of different type, in a few crystals is possible on heating owing to the existence of an order–disorder phase transition at elevated ($\sim$ 1000 °C) temperature. As the ordering process is realized via diffusion, the high-temperature state may be 'frozen' by rapid cooling, and crystals with different degrees of compositional order may be obtained at room temperature. Ordering is known to produce considerable effects on ferroelectric (FE) properties (see the review by Bokov and Rayevsky (1989)), but investigation of the generalities of the effects is hindered by the limited number of known compositionally orderable ferroelectrics. The compositional order–disorder phase transition has been found only in three compounds: $Pb(Sc_{0.5}Nb_{0.5})O_3$, $Pb(Sc_{0.5}Ta_{0.5})O_3$ (Stenger and Burggraaf 1980a) and $Pb(In_{0.5}Nb_{0.5})O_3$ (Bokov *et al* 1983, 1984). These crystals have the perovskite-like structure (Galasso 1969) of $Pb(B'_{0.5}B''_{0.5})O_3$ type and in the ordered state are characterized by regular alternation of B′ and B″ cations. Ordering causes the formation of two B-site sublattices, doubling of the unit cell and the appearance of extra (superlattice) reflections in the x-ray diffraction patterns (Galasso 1969). The integrated intensities of these reflections may be used for measuring the degree of compositional order, which is characterized by long-range order parameter $s = 2p - 1$, where p is the relative quantity of B′ ions in their 'own' sublattice (Stenger *et al* 1979).

0953-8984/93/315491+14$07.50

In some other ferroelectrics a change in the degree of order was reported, indicating the possibility of the order–disorder phase transition, but the transitions themselves were not observed (Bokov and Rayevsky 1989).

The Curie temperature T_C, dielectric permittivity ϵ, the width of the $\epsilon(T)$ maximum at T_C and some other properties change substantially with ordering. $Pb(In_{0.5}Nb_{0.5})O_3$ perovskite shows extraordinary behaviour (Bokov *et al* 1984). In the disordered state it is ferroelectric with a diffuse transition to the paraelectric phase at $T = 60\,°C$. Increase of s leads to the decrease of the FE transition temperature. When s exceeds the critical value s_c the FE transition changes its nature and becomes an antiferroelectric (AFE) one. The temperature of AFE transition T_C is found to increase with s and reaches approximately 200 °C in the ordered crystal. Thus a plot of T_C against s has a minimum.

A thermodynamic treatment made by Bokov *et al* (1983) shows that the Curie temperature in a state with a particular value of s can be calculated from the formula

$$T_C(s) = T_C(0) - As^2 \tag{1}$$

for $s < s_c$ and

$$T_C(s) = T_C(s_c) - B(s^2 - s_c^2) \tag{2}$$

for $s > s_c$, where $T_C(0)$ and $T_C(s_c)$ are the Curie temperatures at $s = 0$ and $s = s_c$, respectively, and A and B are phenomenological parameters.

The usual way to change the value of s is by high-temperature annealing of samples. But very often annealing is accompanied by the transformation of the perovskite structure into the undesirable pyrochlore one, which is non-ferroelectric (Stenger and Burggraaf 1980a, Yasuda and Inagaki 1992), and the time that is needed to change s significantly exceeds the time for complete transformation into the pyrochlore phase. Such behaviour is to a certain degree responsible for the absence of data on compositional ordering effects in some complex perovskites where they are likely to be observed.

In some cases samples with different s have been produced by sintering of ceramics at different temperatures T_s (Stenger *et al* 1979, Stenger and Burggraaf 1980a). The overlapping of annealing and sintering processes that takes place in this method makes it possible to minimize the time of high-temperature treatment.

In this work we studied the compositional order–disorder phase transition and the effects of compositional ordering on the FE properties in $Pb(Yb_{0.5}Nb_{0.5})O_3$ (PYN) complex perovskite-like oxide, which was known as a compositionally ordered antiferroelectric with a Curie point in the range of 280–345 °C (Isupov and Krainik 1964, Kwon and Choo 1991, Kochetkov and Venevtsev 1979, Kurpriyanov and Fesenko 1965, Smolenskii *et al* 1958, Tomashpolskii and Venevtsev 1964). Sintering at different temperatures was used. These results became possible owing to doping of ceramics by a small amount of lithium, which increases the rate of ordering. Some preliminary results of this work have been published earlier (Shonov *et al* 1990).

2. Experimental procedures

2.1. Sample preparation and characterization

Reagent-grade PbO, Yb_2O_3 and Nb_2O_5 were taken as starting materials. To inhibit pyrochlore phase formation, pre-reacted wolframite $YbNbO_4$ was used according to the

method proposed by Swartz and Shrout (1982). First, powders of Yb_2O_3 and Nb_2O_5 were mixed by milling in distilled water and calcined at 1000 °C for 4 h to obtain wolframite. Then it was mixed with PbO to form the perovskite composition. In some cases a small amount of Li_2CO_3 (from 0.5 to 3 wt%), which is known to increase the quality of ceramics and the content of perovskite phase (Groves 1985, Klimov *et al* 1970), was added to the mixture. Unless otherwise mentioned, the amount of Li_2CO_3 in the mixture was 2 wt%. The rest of the procedure was performed in one of two ways. In the first the powder was calcined at 650–800 °C for 24 h. Then it was milled and dried again. Pellets 10 mm in diameter and 1–2 mm thick were fabricated using polyvinyl alcohol (PVA) binder by isostatic pressing at 1.2×10^8 Pa and sintered in a closed alumina crucible at temperatures between 900 and 1140 °C. To limit PbO loss from pellets, a PbO-rich atmosphere was maintained by placing $Pb(Mg_{1/3}Nb_{2/3})O_3$ powder inside the crucible. Unless otherwise mentioned, the temperature of calcination was 750 °C, the time of sintering was 2–3 h at temperatures ranging from 900 to 1070 °C and 0.3–1 h at higher temperatures, and the heating rate before sintering and cooling rate after it were 400 °C h^{-1} and 200–400 °C h^{-1} respectively. The second method of ceramic preparation excluded the stage of calcination at 650–800 °C, but all other procedures were the same.

To denote the samples, abbreviation of compositions with Li will include the letter L and the temperatures of calcination and sintering will be written in parentheses. For example, PYNL (750, 1000) means that the sample of $Pb(Yb_{0.5}Nb_{0.5})O_3$ with Li was fabricated by calcining at 750 °C and subsequent sintering at 1000 °C, and PYN(1100) denotes the sample without Li sintered at 1100 °C without preliminary calcination.

The samples were characterized by x-ray diffraction to determine phase purity, comparing the major x-ray peak intensities for perovskite and pyrochlore phases (Halliyal *et al* 1987). We failed to exclude the pyrochlore phase. The percentage of perovskite phase was in the range of 85 to 98% for the samples sintered at low temperatures (900–1000 °C). The samples sintered at the highest temperatures contained 40–70% of perovskite phase only.

The formation of pyrochlore phase is promoted by a PbO deficiency (Stenger and Burggraaf 1980a), so to investigate the influence of phase purity on ordering and FE properties we produced samples with different proportions of perovskite and pyrochlore phases by means of variation of the amount of $Pb(Mg_{1/3}Nb_{2/3})O_3$ powder in the crucible and by introducing an excess of PbO (up to 20 wt%) into the composition before calcining (in all cases the excess of PbO evaporated during the sintering procedure).

The grain size of ceramics was found to be 1–8 μm. Silver paste was fired on samples as the electrodes for dielectric measurements.

2.2. *Measuring methods*

The structural parameters were studied by x-ray powder diffraction analysis by diffractometer DRON-3 using Cu Kα radiation at room temperature. Unit-cell parameters were calculated from several diffraction peaks. The accuracy of measurements was estimated at about 0.001 Å. The order parameter s was determined by comparing the ratio of the observed intensities of the superstructure reflections to the fundamental structural reflections with the calculated ratio of these intensities in a completely ordered structure (Setter and Cross 1980). That is

$$s^2 = (I_{111}/I_{200})_{\text{observed}}(I_{111}/I_{200})^{-1}_{\text{calc},s=1} \tag{3}$$

with indices referring to the superstructural unit cell of a lattice with compositional but without AFE ordering.

The permittivity and the dielectric loss tangent were measured at a field weaker than 3 V cm^{-1} using an AC bridge while decreasing the temperature at a rate of 2 K min^{-1}. P–E hysteresis loops were observed at 50 Hz by a standard Sawyer–Tower circuit at room temperature.

3. The structure and properties of undoped PYN ceramics

3.1. Experimental results

X-ray diffraction analysis showed that in all PYN samples studied the perovskite subcell had a monoclinic distortion. For PYN(750, 900) the lattice parameters were found to be $a = c = 4.165$ Å, $b = 4.110$ Å, $\beta = 90.55°$. Two sets of superstructure reflections due to antiparallel cation displacements and to B-site cation ordering were clearly observed. The x-ray diffraction pattern of PYN(750, 900) was similar to that reported by Kwon and Choo (1991) for PYN(900, 1120). The crystal symmetry of PYN(750, 900) studied in this work was therefore orthorhombic with lattice parameters $A = 5.861$ Å, $B = 8.220$ Å and $C = 5.918$ Å.

When the sintering temperature T_s increases, the crystal symmetry of the perovskite phase remains unchanged but the compositional order parameter s slightly decreases (the structure characteristics of selected PYN samples are listed in table 1).

Table 1. Structural and ferroelectric parameters[a] of selected $Pb(Yb_{0.5}Nb_{0.5})O_3$ samples.

Compound	t_s (*h*)	s	D (*deg*)	T_C (°C)	Amount of perovskite *phase (%)*
PYN(750, 900)	5	0.78	0.20	286	98
PYN(750, 1135)	2	0.72	0.70	257	63
PYNL(750, 900)	0.2	0.76	0.41	190/249[b]	83
PYNL(900)	3.5	0.75	0.55	190/239[b]	90
PYNL(1000)	2.5	0.67	0.30	102/170/235[b]	77
PYNL(1075)	0.7	0.66	0.38	110/162[b]	84
PYNL(1075)	2.5	0.51	0.18	99	66
PYNL(1075)	3	0.50	0.18	97	58
PYNL(1075)	5	0.53	0.18	98	53
PYNL(1100)	2.5	0.33	0.17	108	62
PYNL(1125)	0.7	0	–	115	52

[a] T_C, Curie temperature; t_s, time of sintering; s, compositional long-range order parameter; D, halfwidth of superstructural (1 1 1) reflection.
[b] Two or three transitions were observed.

Figure 1 shows the temperature dependences of the permittivity ϵ in PYN sintered at different temperatures. The temperature of the $\epsilon(T)$ maximum corresponding to the Curie temperature T_C slightly decreases as T_s increases. Perhaps it is due to the change of s. The samples sintered without preliminary calcination have low ϵ owing to comparatively high porosity.

Figure 2 shows the temperature dependences of ϵ in PYN calcined at different temperatures but sintered at the same T_s. No difference in s was found for these samples (even if it was present, it did not exceed the experimental error). But a reduction of T_C, which was probably caused by small s variation, was observed.

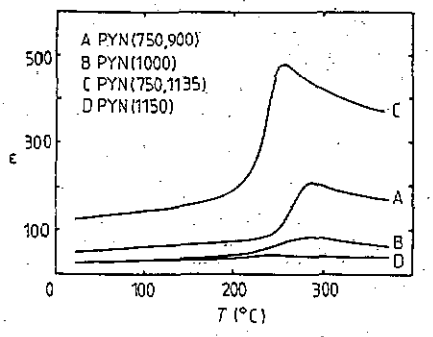

Figure 1. The temperature dependences of permittivity ϵ at 1.6 kHz for PYN ceramics sintered at different temperatures. The time of sintering was 5 h at 900 °C and 2 h at other temperatures.

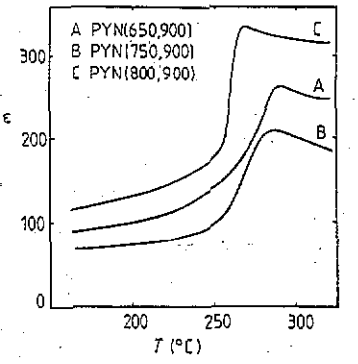

Figure 2. The temperature dependences of permittivity at 1.6 kHz for PYN ceramics calcined at different temperatures.

3.2. Discussion

The absence of a strong relationship between s and T_s for PYN may be explained by one of two assumptions: (i) the compositional order–disorder phase transition in the compounds studied is absent or takes place only at a temperature much higher than the sintering temperature used; (ii) the ordered perovskite structure is formed in the course of heating before the sintering (in particular, during the calcination) at comparatively low temperatures $T < T_s$. The time of sintering is too small to change s considerably because of the small rate of ordering. As a result, the material after sintering has an s value that is the equilibrium one at the calcination temperature (or some temperature $T \sim 700$–800 °C if calcination was not performed).

We tried to promote the disordering process in the course of sintering by increasing T_s, to achieve the disordered state by increasing the sintering time or by decreasing the time during which the sample was heated up to the sintering temperature, but without success. In all cases the perovskite structure was converted into the pyrochlore one completely.

4. The structure and properties of Li-doped ceramics

4.1. Experimental results

X-ray analysis of PYNL samples sintered at comparatively low temperatures (900–1075 °C) confirmed the existence of orthorhombic symmetry analogous to that of the undoped samples. But the structure and properties of PYNL ceramics were found to be strongly influenced by the sintering conditions.

The sintering time t_s was varied in the range of 0.2–48 h. If the sintering temperature T_s was sufficiently high (more than approximately 1000 °C), the decrease of the intensities of superstructural reflections due to compositional ordering with increasing t_s was observed before they settled at steady values (see, for example, the data concerning PYNL(1075) in table 1). These steady values decreased gradually when T_s increased. The effect is evident in figure 3, where the development of one of the superstructural reflections is shown. The compositional order parameter s determined from the settled steady reflection intensities using formula (3) is plotted against T_s in figure 4. The increase in T_s leads to the decrease

of s, indicating the compositional order–disorder phase transition at the temperature T_t where the s value becomes zero. A jump of s value at T_t was not observed and probably the transition is of second order.

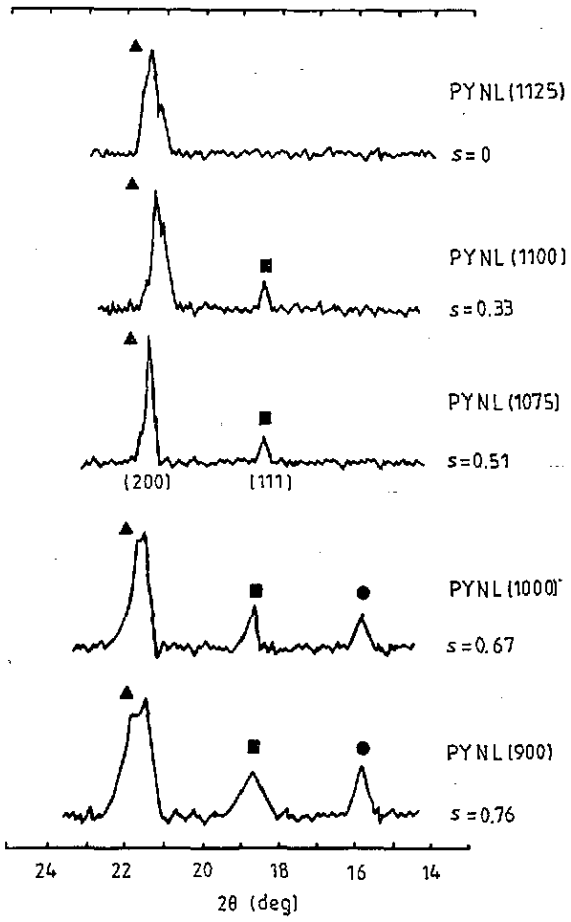

Figure 3. Selected x-ray diffraction patterns of PYNL sintered at *different temperatures:* (▲) *fundamental reflections;* (■) *superlattice* reflections due to the compositional ordering; (●) superlattice reflections due to the antiferroelectric ordering.

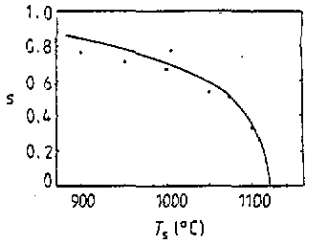

Figure 4. The temperature dependences of *compositional order parameter s for* PYNL ceramics: (●) experimentally measured; (——) calculated using Kirkwood's method.

High accuracy in determining s in the vicinity of T_t could not be achieved because of the small intensities of superstructural reflections. Hence we could not determine the T_t value exactly as well as the order of phase transition by the x-ray diffraction method. From the Curie temperature T_C versus T_s dependence (see next section) T_t was found to be equal to 1120 °C.

The temperature dependence of s calculated for the perovskite structure studied within the scope of Kirkwood's method (Bokov and Rayevsky 1989) is shown in figure 4 by the full curve. The agreement between the calculated and experimental data is quite good, and indicates that the variation of s with temperature is adequately described theoretically.

The decrease of s is accompanied by the following structural changes (they are illustrated by figure 3): (i) the superlattice reflections due to antiparallel cation displacements become less intense and disappear when $s < s_c$ where $s_c \approx 0.6$; (ii) the splitting of fundamental reflections decreases when $s > s_c$, indicating the decrease of the monoclinic distortion of the perovskite subcell. When $s < s_c$ the splitting begins to grow, but the symmetry of the distortion changes. The perovskite-type phase was found to be formed by the mixture of monoclinic and rhombohedral phases.

Figure 5 shows the temperature dependences of the permittivity of PYNL ceramics sintered at different temperatures and hence possessing different s. In contrast to the undoped samples, three anomalies in $\epsilon(T)$ curves may be observed in PYNL. The first high-temperature anomaly was found at 238 ± 4 °C. The second low-temperature anomaly was observed at a temperature strongly dependent on T_s. The third anomaly at approximately 170 °C may be observed between the first and the second ones, but only in ceramics sintered at comparatively high temperatures (more than approximately 970 °C).

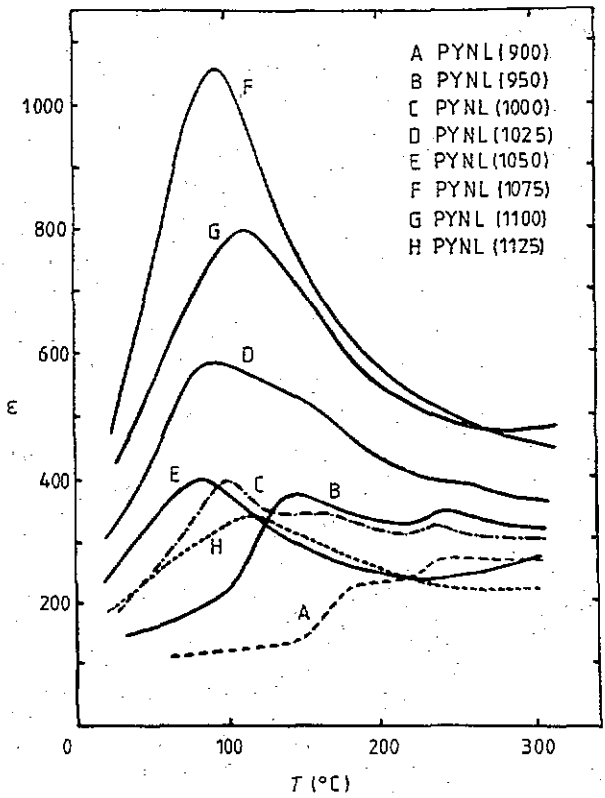

Figure 5. The temperature dependences of permittivity ϵ at 1.6 kHz for PYNL ceramics sintered at different temperatures.

The temperatures of the different $\epsilon(T)$ anomalies are almost independent of sintering time t_s, but their relative intensities depend on t_s dramatically. This dependence is basically different in materials sintered at comparatively high temperatures (more than approximately 970 °C) and at low temperatures. In the first ones the low-temperature anomaly grows when t_s is increased, the other anomalies gradually disappear and the single $\epsilon(T)$ maximum is left at last (see e.g. figure 6(*a*)). The sintering time necessary to complete the process decreases with increasing T_s. For example, it is equal to 0.5 h and 2 h at $T_s = 1125$ °C

and 1075 °C respectively. In the case of ceramics sintered at $T_s \lesssim 970$ °C the existence of the low-temperature anomaly was not apparent, while the two high-temperature anomalies remained even after very long sintering times (compare curves D and E in figure 6(*b*)).

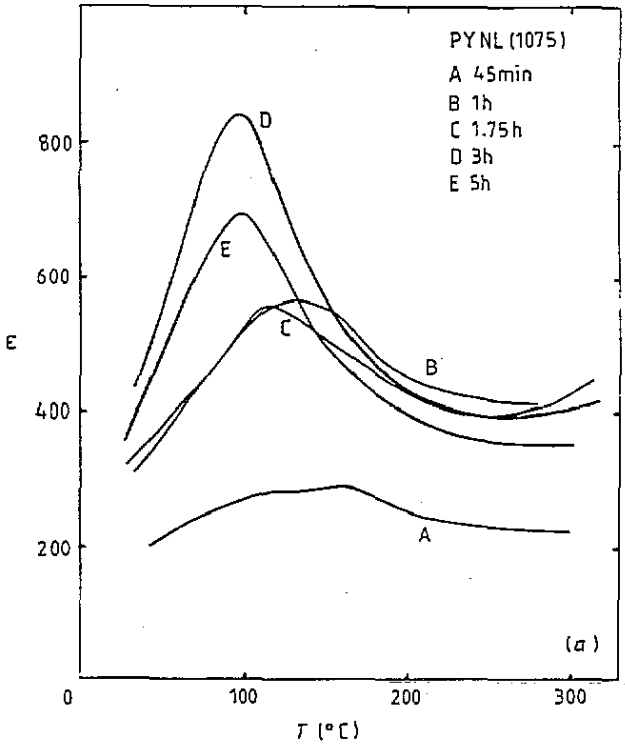

Figure 6. The temperature dependences of permittivity ϵ at 1.6 kHz in PYNL ceramics sintered for different times t_s at (*a*) 1075 °C. Values of t_s are indicated in the keys.

The growth of ϵ at high temperatures, which was observed in some samples, is typical of low-frequency $\epsilon(T)$ curves in lead-containing perovskites, and is connected with the rise of conductance at high temperature. This increase was absent in the curves measured at 1 MHz.

To investigate if the values of s and T_C change during cooling after sintering, we performed special experiments. After sintering at extremely high T_s, samples were quenched by removing the crucible from the furnace. Then they were annealed at 800 °C for 1 h to eliminate mechanical stresses. No distinctions between the properties of quenched and furnace-cooled samples were found, showing that s remains unchanged in the course of cooling.

4.2. Discussion

We assume that the additional $\epsilon(T)$ anomalies in PYNL ceramics result from spatial non-homogeneities of the structure, i.e. the coexistence of regions with different compositional order parameter s. The peculiarities of the formation of non-homogeneities are determined by ordering kinetics as well as solid-state reactions during calcination and sintering.

It is known (Stenger and Burggraaf 1980b, Bokov *et al* 1986) that in ceramics of lead-based complex perovskites isothermal ordering (disordering) proceeds via the formation of regions with different s and hence different T_C. The coexistence of these regions leads to the

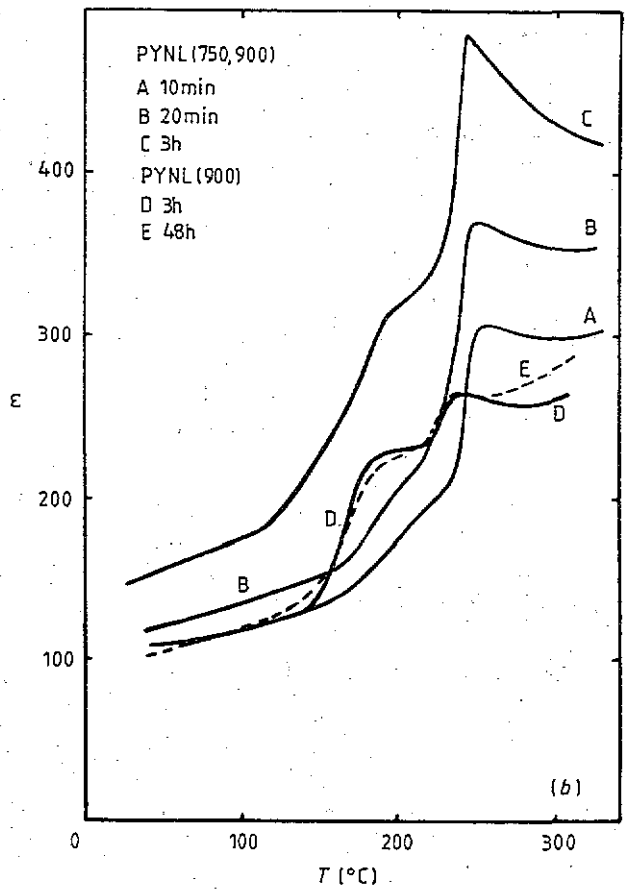

Figure 6. (*Continued*). The temperature dependences of permittivity ϵ at 1.6 kHz in PYNL ceramics sintered for different times t_s at (*b*) 900 °C. Values of t_s are indicated in the keys.

appearance of two successive anomalies in the $\epsilon(T)$ curve. With a change of the fraction of ordered material in the course of time, one of the anomalies becomes stronger and the other gradually decreases, but their temperatures remain almost unchanged. The existence of small regions with different s in the samples with incomplete ordering also causes broadening of x-ray superstructural reflections. When the ordering process is complete and s becomes uniform in the bulk of the sample, one maximum only is left in the $\epsilon(T)$ curve.

The formation of the perovskite structure of lead-containing $Pb(B'B'')O_3$ niobates is a complicated multistage process, with several intermediate products during the solid-state reaction in the temperature range from 500 to 900 °C (Agranovskaia 1960, Dambekalne *et al* 1989, 1992). In the course of the temperature increase, the pyrochlore phase may be formed in the initial stages of reaction, and then it is converted into the perovskite phase at higher temperatures. The intermediate pyrochlore phase is metastable and conversion is possible at all stages of reaction. As a result, in the case of two-step calcination the content of the perovskite phase after the second step (sintering) is higher than after the first one (Dambekalne *et al* 1992). We found that this is true for PYNL samples as well.

The high-temperature $\epsilon(T)$ anomaly in PYNL (at 238 °C) seems to be caused by the regions of perovskite structure synthesized during heating up to sintering temperature and during calcination (if it was performed). As the calcination temperature is significantly lower than T_t, the compositionally ordered structure is formed.

In the case of comparatively low sintering temperatures $T_s \simeq 900$–$970\,^{\circ}C$, the new regions of perovskite phase formed by sintering give rise to the second (low-temperature) anomaly, which increases gradually with the content of the perovskite phase (see figure 6(*b*)). For example, PYNL sintered for 0.3 h at 900 °C (curve B in figure 6(*b*)) contained 83% of the perovskite phase, while after 3 h of sintering (curve C in figure 6(*b*)) this percentage increased up to 95%. The growth of the low-temperature anomaly is over when solid-state reaction at T_s ceases. The perovskite regions formed during the calcination (or heating) have an s value that is a non-equilibrium one at T_s, but the rate of s change is very small owing to low T_s, the process of disordering cannot develop and the ceramics remain non-homogeneous.

The increase of T_s increases the rate of disordering and permits the ceramics to reach an equilibrium homogeneous state at T_s along with sintering. As can be seen in figure 6(*a*) the evolution of $\epsilon(T)$ anomalies in this case is in good agreement with the picture described above for the disordering process. The high-temperature anomaly disappears when the process is over.

The third intermediate $\epsilon(T)$ anomaly (at $\sim 170\,^{\circ}C$) may be attributed to the effect of perovskite regions synthesized during heating before sintering but at comparatively high temperatures.

The existence of spatially non-homogeneous disorder is confirmed by the fact that the x-ray superstructural reflections due to compositional ordering in PYNL samples with several $\epsilon(T)$ anomalies were broadened much more in comparison to those obtained for samples with one anomaly (see table 1).

It should be noted that in non-homogeneous material the value of s calculated from formula (3) is the average over the sample's bulk. But the non-homogeneities could not be eliminated only in the samples with high s where the difference in s of different regions was small and the measured s was close to the equilibrium value. So we can consider that figure 4 shows equilibrium s value at T_s.

In undoped PYN materials the formation of perovskite phase becomes complete during calcination, the rate of ordering is small even at high T_s and the homogeneous structure with equilibrium s value for the calcination temperature can be found after sintering independently of T_s. In this case the sole $\epsilon(T)$ maximum is observed at a temperature dependent on calcination temperature (see figures 1 and 2).

The explanations above are true if we conclude that in the course of PYNL ceramic synthesis the ordered perovskite structure is formed, i.e. the structure that is the equilibrium one at the temperature of formation. This is in contrast to the processes in crystals, e.g. $Pb(Sc_{0.5}Nb_{0.5})O_3$ and $Pb(Sc_{0.5}Ta_{0.5})O_3$, the latter growing disordered at any temperature, even lower than T_t (Bokov *et al* 1987).

Figure 7 shows the Curie temperature of PYNL ceramics having equilibrium s value at high temperature T_s plotted against T_s. In view of the insights above, T_C in this figure was determined as the temperature of the $\epsilon(T)$ maximum if there were no other $\epsilon(T)$ anomalies and as the temperature of the low-temperature anomaly in other cases. Every experimental point in figure 7 is the average value of 3–8 samples containing different amounts of Li. The standard deviation of T_C value was 2–5 °C. No difference in T_C for PYNL samples with given s, but different content of Li, different porosity or different pyrochlore phase impurity, was observed.

Figure 7 shows that the effect of T_s on T_C disappears when $T_s > 1120\,^{\circ}C$. It means that the compositional order–disorder phase transition takes place at this temperature.

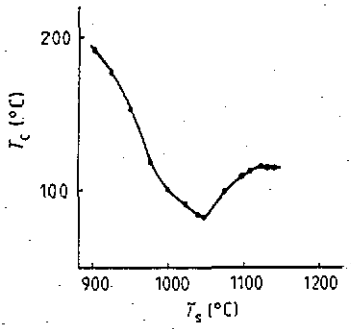

Figure 7. The Curie temperature as a function of sintering temperature T_s in PYNL.

5. The effect of compositional ordering on ferroelectric properties

The analogy of dielectric and structural behaviour in the samples under consideration and $Pb(In_{0.5}Nb_{0.5})O_3$ crystals (Bokov *et al* 1983, 1984) suggests the idea that the phase transition in PYNL is antiferroelectric when $s > s_c$ and ferroelectric when $s < s_c$, i.e. a triple point of FE–AFE–PE type takes place at $s = s_c$. This analogy is confirmed by the following experimental data:

(i) The superlattice reflections due to antiparallel cation displacements disappear and the orthorhombic structure typical of AFE perovskites changes to the rhombohedral one typical of FE perovskites when s becomes less than s_c (see section 4).

(ii) FE hysteresis loops typical of ferroelectrics with diffuse phase transitions (Smolenskii *et al* 1971) are observed for samples with $s < s_c$, but in the case of $s > s_c$, the $P(E)$ relation is linear (figure 8).

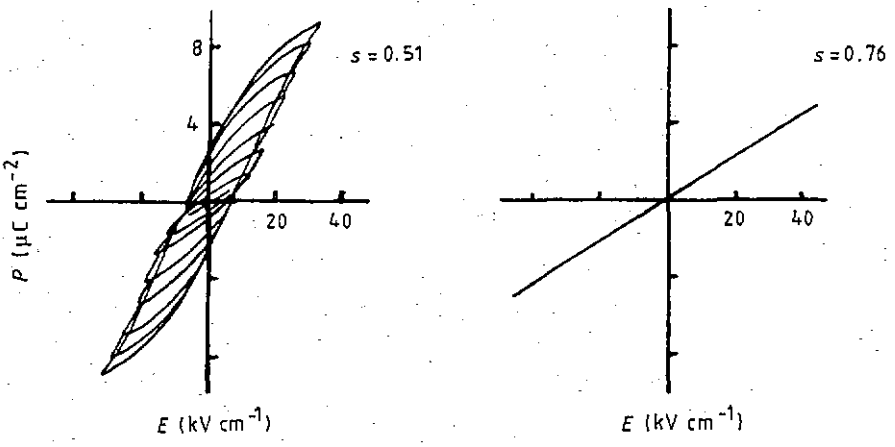

Figure 8. Polarization P versus electric field E relation of PYNL ceramics with different compositional order parameter s.

(iii) The DC bias field E shifts T_C towards higher temperatures and decreases the peak value of ϵ at T_C when $s < s_c$ (figure 9), but does not affect them if $s > s_c$. The value of dT_C/dE of PYNL (7.7 K cm kV^{-1} when $s = 0.51$) is a little larger than in other ferroelectrics

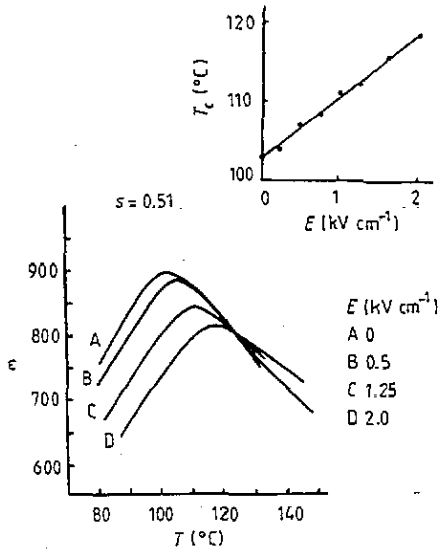

Figure 9. The temperature dependences of permittivity ϵ at 1.6 kHz for different DC bias fields E in partially ordered PYNL(1075) ($s = 0.51$). Inset: the shift in the Curie temperature T_C with increasing E.

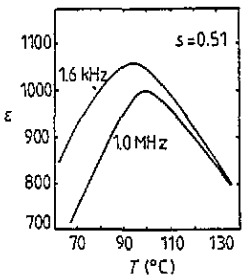

Figure 10. The temperature dependences of permittivity ϵ at different frequencies for partially ordered PYNL(1075) ($s = 0.51$).

with diffuse phase transitions (3.5 K cm kV^{-1} in $Pb(Mg_{1/3}Nb_{2/3})O_3$ (Bokov and Mylnikova 1961) and 3.9 K cm kV^{-1} in $Sr_{0.67}Ba_{0.33}Nb_2O_6$ (Glass 1969)).

(iv) The temperature of peak permittivity shifts upwards with increasing frequency, and strong dielectric dispersion occurs over the transition region if $s < s_c$ (figure 10). Such behaviour is usual for ferroelectrics with diffuse phase transitions (Smolenskii *et al* 1971). But if $s > s_c$ neither shift nor dispersion is observed.

(v) The maximum of tan $\delta(T)$ is observed in the region of the Curie temperature if $s < s_c$ and is absent in the other case (figure 11), indicating the change from FE to AFE phase transition (Bokov and Shonov 1990).

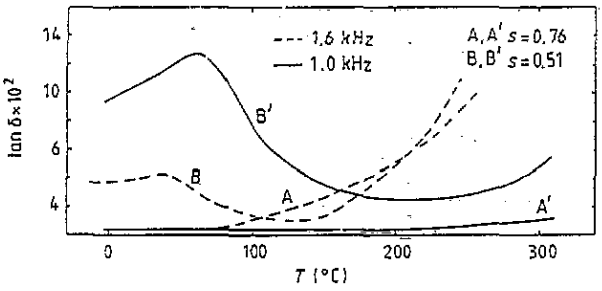

Figure 11. The temperature dependences of dielectric loss tangent tan δ for PYNL ceramics with different compositional order parameter.

(vi) As s decreases, the magnitude of the permittivity generally grows (figure 5). But high-temperature sintering promotes the formation of the non-ferroelectric pyrochlore phase and increases the porosity. The variation in the magnitude of ϵ as a function of T_s is defined by two concurrent trends, namely: the growth of ϵ due to s decrease and the decrease of ϵ due to the pyrochlore content and porosity rise. These seem to be the reason for the non-monotonicity of the $\epsilon(T_s)$ dependence.

To study the validity of equations (1) and (2) for PYNL, the T–s phase diagram was plotted (figure 12). As can be seen, these equations are in good agreement with the experimental results. The quadratic dependence of T_C on s is violated only in the vicinity of the boundary between FE and AFE phases (triple point). Perhaps this is due to the coexistence of FE and AFE phases there. The constants in equations (1) and (2) were evaluated from figure 12 to give $T_C(0) = 116\,°C$, $T_c(s_c) = 78\,°C$, $s = 0.645$, $A = 92\,°C$, $B = -704\,°C$. The calculated Curie temperature of fully ordered PYNL ($T_C(1)$) was equal to 489 °C.

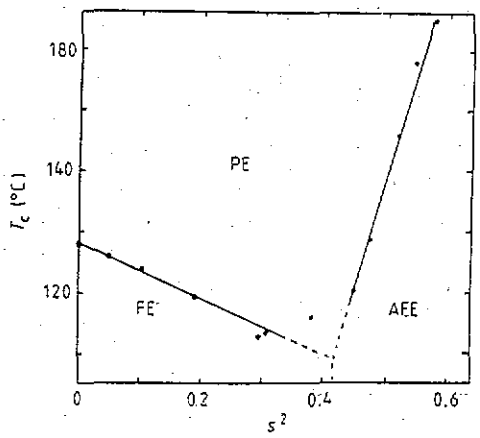

Figure 12. The phase diagram (T–s plot) of PYNL ceramics.

6. Conclusion

The compositional order–disorder phase transition at $T = 1120\,°C$, the T–s phase diagram and the influence of compositional disorder on FE properties were studied in Li-doped $Pb(Yb_{0.5}Nb_{0.5})O_3$ ceramics. In pure ceramics such investigations could not be made because of the absence of the possibility to change the s value owing to a very low rate of ordering. It is not clear if the difference between the values of T_t, T_C and other parameters in doped and undoped ceramics is large, but we believe that it is not large in comparison with the effects caused by compositional ordering. This opinion is confirmed by the experimental data showing that the influence of doping on s in ceramics sintered at low temperatures is small, and the differences in the T–s phase diagrams for ceramics with different Li concentrations is unnoticeable. Besides, it is known (Klimov *et al* 1970) that in a cognate $Pb(Fe_{0.5}Nb_{0.5})O_3$ ceramic in which compositional ordering effects are absent, Li additions shift down T_C by 15 °C at the most.

Two anomalies in the $\epsilon(T)$ curve of PYN similar to those obtained in this work have been observed in some other papers (Tomashpolskii and Venevtsev 1964, Isupov and Krainik 1964). The authors of these papers assumed that the anomalies were caused by two different phase transitions. But it was not clear why in other works (Kochetkov and Venevtsev 1979, Pronin *et al* 1982) only one anomaly (maximum at the Curie temperature) has been found. Our results show that the most probable cause of the existence of two anomalies is spatial non-homogeneities of compositional disorder dependent on the peculiarities of ceramic preparation. The large spread in T_c values for PYN ceramics fabricated by different researchers (from 280 to 345 °C) may be explained by differences in s.

References

Agranovskaia A I 1960 *Izv. Akad. Nauk. SSSR Ser. Fiz.* **24** 1275

Bokov A A and Rayevsky I P 1989 *Ferroelectrics* **90** 125

Bokov A A, Rayevsky I P and Smotrakov V G 1983 *Fiz. Tverd. Tela* **25** 2025

—— 1984 *Fiz. Tverd. Tela* **26** 2824

Bokov A A, Rayevsky I P, Smotrakov V G and Prokopalo O I 1986 *Phys. Status Solidi* a **93** 411

Bokov A A, Rayevsky I P, Smotrakov V G and Zaitsev S M 1987 *Kristallografiya* **32** 1301

Bokov A A and Shonov V Y 1990 *Ferroelectrics* **108** 237

Bokov V A and Mylnikova I E 1961 *Sov. Phys.–Solid State* **3** 613

Dambekalne M, Brante I, Antonova M and Sternberg A 1992 *Ferroelectrics* **131** 67

Dambekalne M, Brante I and Sternberg A 1989 *Ferroelectrics* **90** 1

Galasso F S 1969 *Structure, Properties and Preparation of Perovskite-type Compounds* (Oxford: Pergamon)

Glass A M 1969 *J. Appl. Phys.* **40** 4699

Groves P 1985 *Ferroelectrics* **65** 67

Halliyal A, Kumar U, Newnham R E and Cross L E 1987 *Am. Ceram. Soc. Bull.* **66** 671

Isupov V A and Krainik N N 1964 *Fiz. Tverd. Tela* **6** 3713

Klimov V V, Didkovskaya O S and Zvonik V A 1970 *Neorg. Mater.* **6** 182

Kochetkov V V and Venevtsev Y N 1979 *Izv. Akad. Nauk. SSSR Ser. Neorg. Mater.* **15** 1833

Kupriyanov M F and Fesenko E G 1965 *Kristallografiya* **10** 246

Kwon J R and Choo W K 1991 *J. Phys.: Condens. Matter* **3** 2147

Pronin I P, Isupov V A, Parfenova N N and Zaitseva N V 1982 *Ferroelectrics and Piezoelectrics* (Kalinin: Kalinin State University) p 125

Setter N and Cross L E 1980 *J. Mater. Sci.* **15** 2478

Shonov V Y, Bokov A A, Rayevsky I P, Kogan V A and Kuprianov M F 1990 *Proc. Int. Conf. Electronic Ceramics—Production and Properties* (Riga) p 116

Smolenskii G A, Agranovskaya A I, Popov S N and Isupov V A 1958 *Sov. Phys.–Tech. Phys.* **3** 1981

Smolenskii G A, Bokov V A, Isupov V A, Krainik N N, Pasinkov R E and Shur M S 1971 *Ferroelectrics and Antiferroelectrics* (Leningrad: Nauka)

Stenger C G F and Burggraaf A J 1980a *Phys. Status Solidi* a **61** 275

—— 1980b *Phys. Status Solidi* a **61** 653

Stenger C G F, Scholten F L and Burggraaf A J 1979 *Solid State Commun.* **32** 989

Swartz S L and Shrout T R 1982 *Mater. Res. Bull.* **17** 1245

Tomashpolskii Y Y and Venevtsev Y N 1964 *Fiz. Tverd. Tela* **6** 2998

Yasuda N and Inagaki H 1992 *Ferroelectrics* **126** 115